NUMERICAL SIMULATION OF ELONGATION OF SAND SPIT ON SEABED WITH DIFFERENT WATER DEPTHS AND SLOPES

Toshiro San-nami[1], Takaaki Uda[2], Masumi Serizawa[1] and Shiho Miyahara[1]

The elongation of a sand spit on a seabed with different water depths and slopes was numerically simulated using the BG model (a three-dimensional model for predicting beach changes based on Bagnold's concept). The examples of sand spits and a pond enclosed by a barrier were examined first using aerial photographs and bathymetric survey maps. The formation of a sand spit and a barrier was predicted using the BG model under the conditions that the water depths where a sand spit is formed were changed to 5, 10, 15, and 20 cm in a model scale of 1/100, and that the seabed slopes were changed to 1/50, 1/40, 1/30, and 1/20. The difference in the form of a sand spit and a barrier formed under these conditions was explained and compared with the natural sand spits and a barrier.

Keywords: Sand spit; barrier; beach changes; BG model; predictive model

INTRODUCTION

A sand spit is generally formed at a location where the shoreline orientation abruptly changes. The shoreline around a sand spit has a large curvature and dynamically changes in accordance with the sand supply from the upcoast, and therefore, the prediction of topographic changes around the sand spit was difficult compared with that of a statically stable beach. In recent studies of the development of the sand spit, Ashton et al. (2001) showed that shoreline instability may develop and the sand spit can emerge from a small perturbation under oblique wave incidence with the angle between the direction normal to the shoreline and the wave direction being larger than 42°. Serizawa and Uda (2011) numerically simulated the development of the sand spit using the BG model (a three-dimensional model for predicting beach changes based on Bagnold's concept), and their results were compared with the results of a movable bed experiment with a model scale of 1/100 under the conditions that the coastline orientation abruptly changes on the shallow seabed and a steep slope extends along the corner where the coastline orientation changes. They successfully explained the formation of a sand spit and a barrier. However, in their study, the effects of the change in water depth of the flat shallow seabed and the change in slope of the sand accumulation zone on the formation of the sand spit have not yet been fully investigated. In this study, the effects of the differences in the water depth and seabed slope on the elongation of a sand spit or a barrier were investigated using the BG model, together with the investigation of the examples of a sand spit and a barrier formed along the west Izu coast facing Suruga Bay.

EXAMPLES OF SAND SPIT AND BARRIER ON WEST IZU COAST

Typical examples of the sand spit and a barrier can be observed on the west coast of Izu Peninsula, facing Suruga Bay, as shown in Fig. 1. The seabed topography in the rectangular area in Heda in Fig. 1 is shown in Fig. 2. At the mouth of Heda Bay, a recurved sand spit named Mihama Point of 650 m length extends. The bathymetry in the rectangular area of Heda Bay shown in Fig. 2 is drawn in Fig. 3. The water depth at the tip of the sand spit is as much as 30 m, which is much larger than the depth of closure h_c = 10 m in this area, and the slope surrounding the sand spit is very steep.

North of Mihama Point, a barrier is located 2.2 km north of the sand spit (Figs. 2 and 4), separating Myojin Pond from Suruga Bay, and further north, another recurved sand spit of Osezaki Point with a 650 m length extends 3.3 km north of the pond (Figs. 1 and 5). The development of a sand spit and a barrier, as shown in these figures, strongly suggests that the water depth and the seabed slope of the sand deposition zone where the sand spit or a barrier extends are key factors for the formation of the sand spit and the barrier.

[1] Coastal Engineering Laboratory Co., Ltd., 1-22-301 Wakaba, Shinjuku, Tokyo 160-0011, Japan
[2] Public Works Research Center, 1-6-4 Taito, Taito, Tokyo 110-0016, Japan

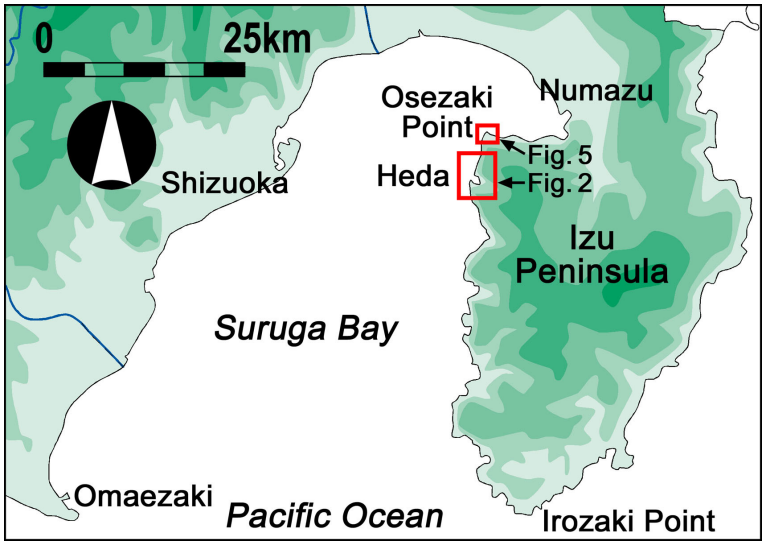

Figure 1. Location of Heda and Osezaki Points on west coast of Izu Peninsula.

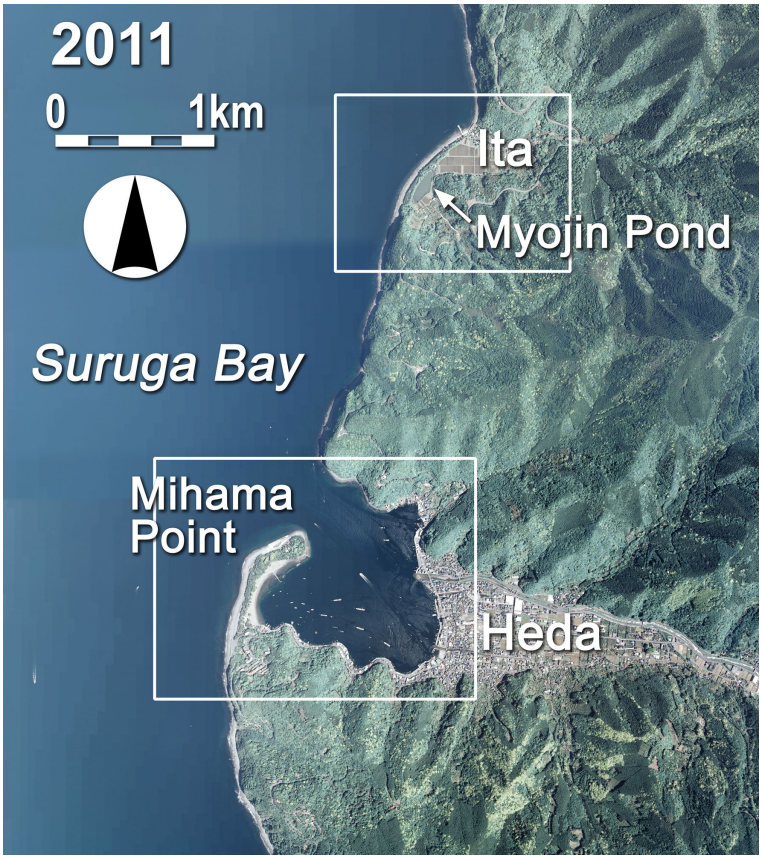

Figure 2. Aerial photograph of Mihama Point and Myojin Pond.

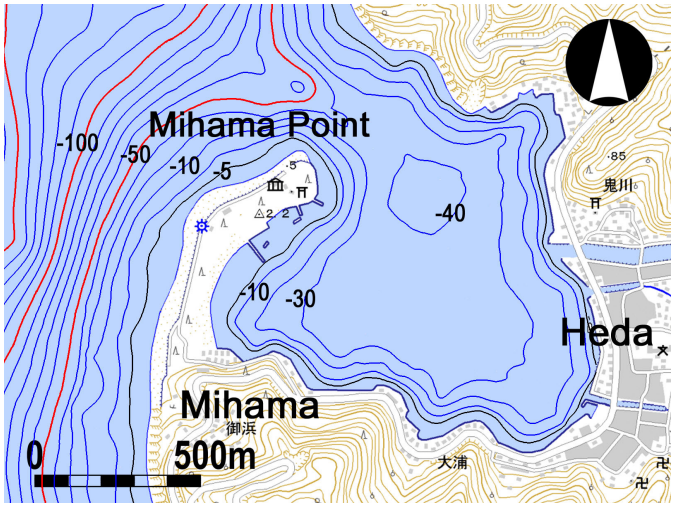

Figure 3. Bathymetry around Mihama Point.

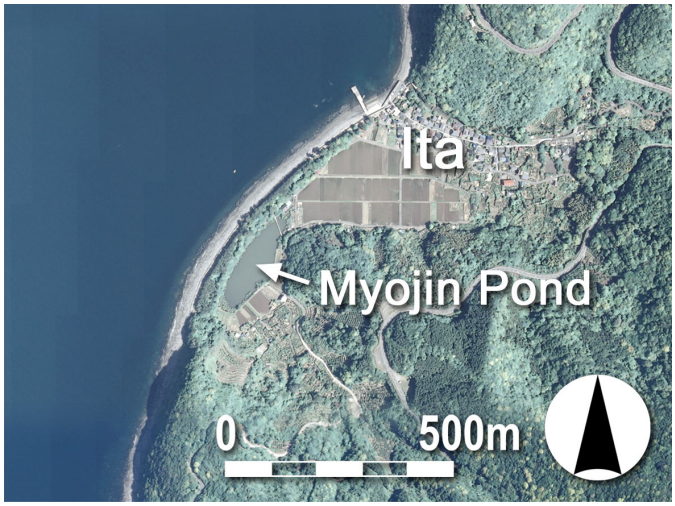

Figure 4. Aerial photograph of Myojin Pond.

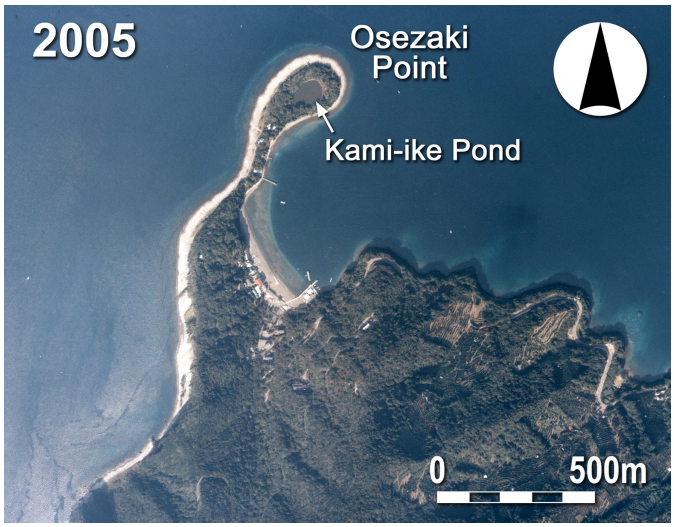

Figure 5. Aerial photograph of Osezaki Point taken in 2005.

NUMERICAL SIMULATION USING THE BG MODEL

Model

The BG model proposed by Serizawa and Uda (2011) with an additional term from Ozasa and Brampton (1980) was used in the numerical simulation. The fundamental equations are given as

$$\vec{q} = C_0 \frac{K_s P}{\tan\beta_c} \left\{ \begin{array}{l} K_n \left(\tan\beta_c \vec{e_w} - |\cos\alpha| \ \vec{\nabla Z} \right) \\ + \left\{ (K_s - K_n)\sin\alpha - \dfrac{K_2}{\tan\bar{\beta}} \dfrac{\partial H}{\partial s} \right\} \tan\beta \vec{e_s} \end{array} \right\} \qquad \left(-h_c \le Z \le h_R\right) \quad (1)$$

$$P = \rho u_m^3 \tag{2}$$

$$u_m = \frac{H}{2}\sqrt{\frac{g}{h}} \tag{3}$$

where $\vec{q} = \left(q_x,\ q_y\right)$ is the net sand transport flux, Z (x, y, t) is the elevation with reference to the still water level, n and s are the local coordinates taken along the directions normal (shoreward) and parallel to the contour lines, K_s and K_n are the coefficients of longshore and cross-shore sand transport, respectively, $\vec{\nabla Z} = \left(\partial Z/\partial x,\ \partial Z/\partial y\right)$ is the slope vector, $\vec{e_w}$ is the unit vector of the wave direction, $\vec{e_s}$ is the unit vector parallel to the contour lines, α is the angle between the wave direction and the direction normal to the contour lines, $\tan\beta = \left|\vec{\nabla Z}\right|$ is the seabed slope, $\tan\beta_c$ is the equilibrium slope, $\tan\beta\vec{e_s} = \left(-\partial Z/\partial y,\ \partial Z/\partial x\right)$, K_2 is the coefficient of the term given by Ozasa and Brampton (1980), $\partial H/\partial s = \vec{e_s}\cdot\vec{\nabla H}$ is the longshore gradient of the wave height H measured parallel to the contour lines, and $\tan\bar{\beta}$ is the characteristic slope of the breaker zone. In addition, C_0 is the coefficient transforming the immersed weight expression into the volumetric expression ($C_0 = 1/\{(\rho_s - \rho)g(1-p)\}$, where ρ is the density of seawater, ρ_s is the specific gravity of sand particles, p is the porosity of sand, and g is the acceleration of gravity), u_m is the amplitude of the seabed velocity due to the orbital motion of waves, h_c is the depth of closure, and h_R is the berm height.

The wave field was calculated using the energy balance equation given by Mase (2001) with the term of wave dissipation due to wave breaking given by Dally et al. (1984). In the calculation of the wave field on land, the imaginary depth h' was given by Eq. (4) between the minimum depth h_0 and the berm height h_R.

$$h' = \left(\frac{h_R - Z}{h_R + h_0}\right)^r h_0 \qquad (r = 1) \qquad \left(-h_0 \le Z \le h_R\right) \tag{4}$$

In addition, at locations higher than the berm height, the wave energy was set to be 0. The wave field was calculated every 10 steps of the calculation of topographic changes. In the numerical simulation of beach changes, the sand transport and continuity equations ($\partial Z/\partial t + \nabla \bullet \vec{q} = 0$) were solved on the x-y plane by the explicit finite-difference method.

In estimating the intensity of sand transport near the berm top and at the depth of closure, the intensity of sand transport was linearly reduced to 0 near the berm height and the depth of closure to prevent sand from being deposited in the zone higher than the berm height and the beach from being eroded in the zone deeper than the depth of closure using the procedure given by Uda et al. (2012).

Calculation Conditions

In the calculation of the elongation of the sand spit, the water depths of the shallow seabed where the sand spit elongates were changed to 5, 10, 15, and 20 cm in Cases 1-4, respectively, with a model scale of 1/100. The seabed slopes of the sand deposition zone were also changed to 1/50, 1/40, 1/30, and 1/20 in Cases 5-8, respectively. Case 1 is the same as the results of Serizawa and Uda (2011), and it gives the reference for the other cases. The incident wave height was H_i = 4.6 cm, and the wave period T = 1.27 s. Waves were obliquely incident with an angle of 20° normal to the initial shoreline. The depth of closure was given as h_c = 2.5H, where H is the wave height at a point. The berm height and equilibrium slope of sand were assumed as 5 cm and 1/5, respectively, based on the experimental

results along with the angle of the slope of sand of 1/2. The calculation domain was discretized by meshes of 20 cm, and the 8 hr of calculation (8×10^4 steps) was carried out using the time intervals of $\Delta t = 10^{-4}$ hr. Table 1 shows the calculation conditions. The calculation results are shown with the same model scale of 1/100, so that it is easy to compare the results of this study with those given by Serizawa and Uda (2011), in which the formation of a spit with a model scale of 1/100 was predicted. The numbers in parentheses in Table 1 correspond to the experimental conditions.

Table 1. Calculation conditions.

Wave conditions	Incident waves: H_I = 4.6 m (4.6 cm), T = 12.7s (1.27 s), wave direction θ_I = 20° relative to normal to initial shoreline
Berm height	h_R = 5 m (5 cm)
Depth of closure	$h_c = 2.5H$ (H: wave height)
Equilibrium slope	$\tan\beta_c$ = 1/5
Angle of repose slope	$\tan\beta_g$ = 1/2
Coefficients of sand transport	Coefficient of longshore sand transport K_s = 0.045 Coefficient of Ozasa and Brampton (1980) term $K_2 = 1.62K_s$ Coefficient of cross-shore sand transport $K_n = 0.1\ K_s$
Mesh size	$\Delta x = \Delta y$ = 20 m (20 cm)
Time intervals	$\Delta t = 10^{-3}$ hr (10^{-4} hr)
Duration of calculation	80 (8) hr (8×10^4 steps)
Boundary conditions	Shoreward and landward ends: $q_x = 0$, right and left boundaries: $q_y = 0$
Calculation of wave field	Energy balance equation (Mase, 2001) •Term of wave dissipation due to wave breaking: Dally et al. (1984) model •Wave spectrum of incident waves: directional wave spectrum density obtained by Goda (1985) •Total number of frequency components N_F =1 and number of directional subdivisions N_θ = 8 •Directional spreading parameter S_{max} = 75 •Coefficient of wave breaking K = 0.17 and Γ = 0.3 •Imaginary depth between minimum depth h_0 and berm height h_R : h_0 = 2 m (2 cm) •Wave energy = 0 where $Z \geq h_R$ •Lower limit of h in terms of wave decay due to breaking Φ: 0.7 m (0.7 cm)

CALCULATION RESULTS

Formation of Sand Spit on a Flat Bottom with Constant Depth

Figures 6-9 show the initial topography with a flat bottom in the sand deposition area and the results after an eight-hour wave action of Cases 1-4, in which the water depth of the shallow seabed is constant at 5, 10, 15, or 20 cm, respectively. In Case 1, the sand spit rapidly extended along the marginal line of the shallow seabed forming a barrier, because the water depth of the sand deposition zone is much smaller than the depth of closure h_c = 12 cm, and it connected with the other side, leaving a shallow lagoon inside up to 2 hr. After 4 hr, the width of the sand bar increased because of the sand deposition to the deeper zone from the left boundary, while forming a steep slope.

In Case 2 (h_0 = 10 cm), the elongation velocity of the sand spit decreased compared with that in Case 1 because of the increase in the volume of the sand deposition zone. Furthermore, because the wave energy incident to the shallow seabed increased owing to the increase in water depth, the curvature at the tip of the sand spit also increased. As a result, the tip of the sand spit approached very close to the X-axis after 4 hr, and connected at X = 14 m after 8 hr. In addition, detailed investigation of the topography on the opposite side against the sand spit after 4 hr shows that a cuspate foreland was also formed owing to the wave-sheltering effect of the sand spit itself. Thus, in Case 2 with a greater depth of the flat bottom, the area of the lagoon behind the barrier markedly decreased compared with that in Case 1 because of the oblique elongation of the sand spit.

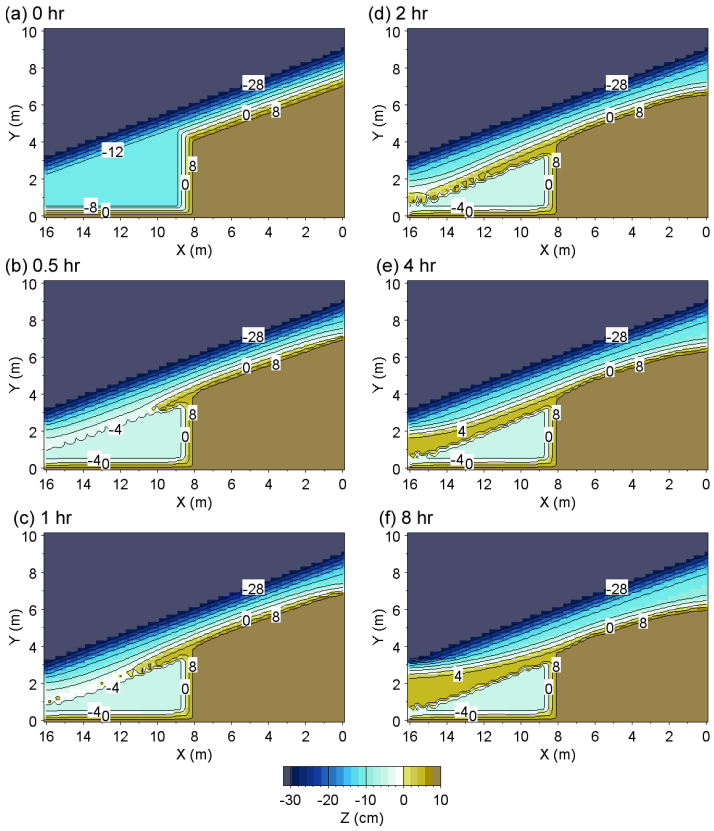

Figure 6. Formation of sand spit on flat sea bottom with 5 cm depth (Case 1).

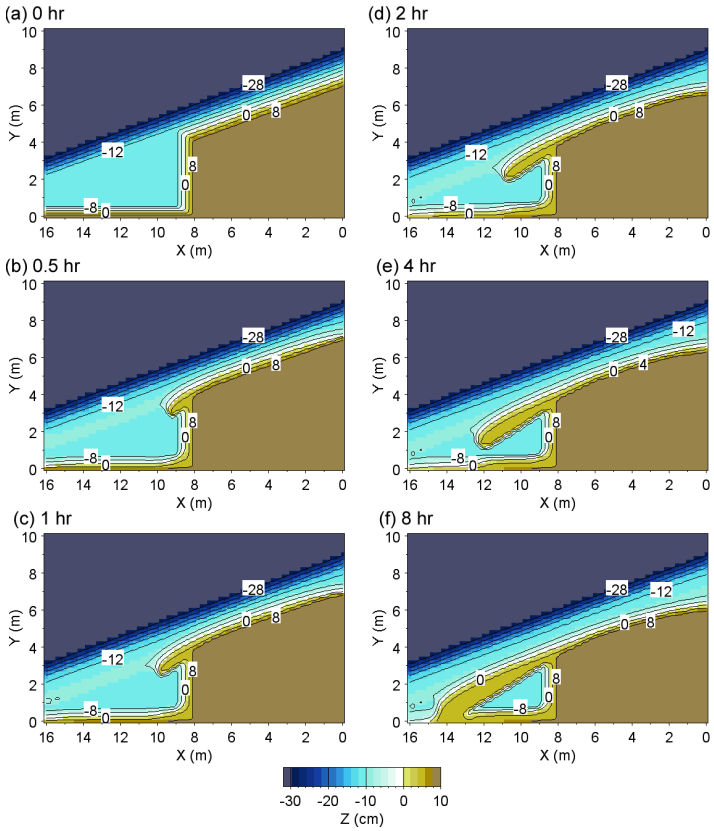

Figure 7. Formation of sand spit on flat sea bottom with 10 cm depth (Case 2).

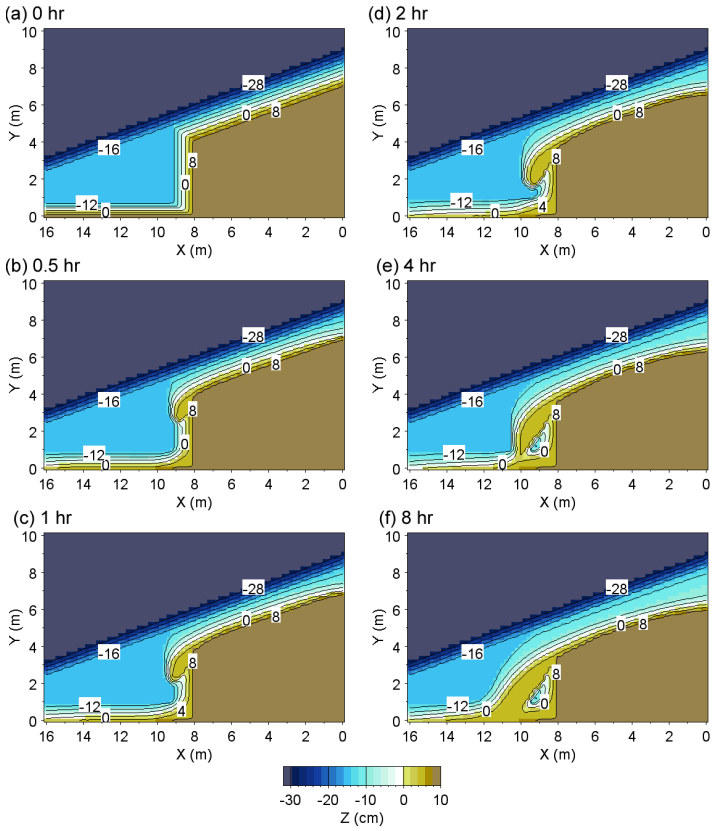

Figure 8. Formation of sand spit on flat sea bottom with 15 cm depth (Case 3).

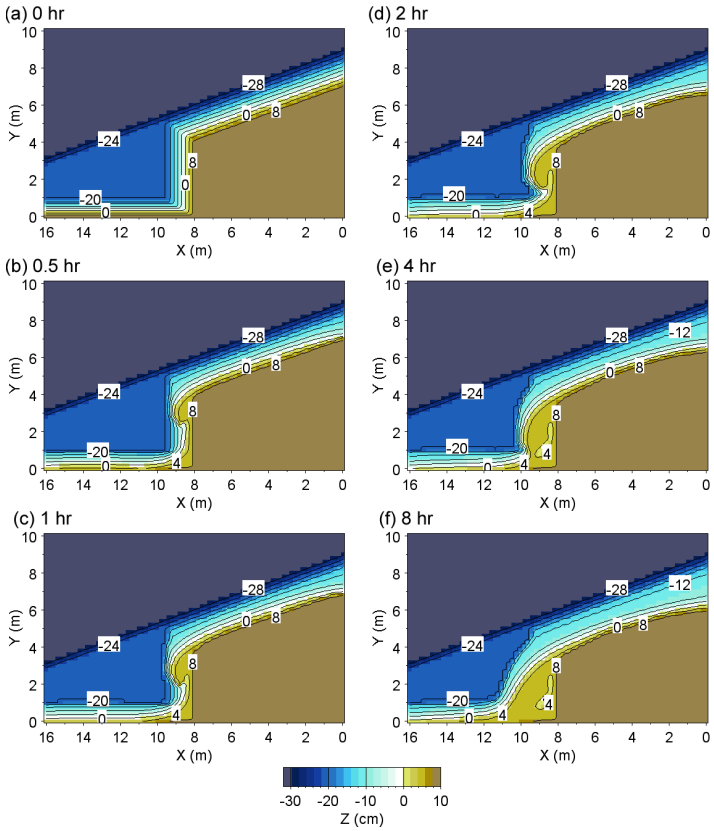

Figure 9. Formation of sand spit on flat sea bottom with 20 cm depth (Case 4).

In Case 3 (h_0 = 15 cm), the elongation velocity of the sand spit further decreased with the increase in water depth, and the length of the sand spit markedly decreased because of succesive sand deposition into the deeper zone. When the water depth of a flat bottom is greater than h_c in the offshore zone, part of the sand transported from the upcoast falls into the zone deeper than h_c and such sand cannot be transported again by wave action, implying that an additional volume of sand is required for the sand spit to be formed. It is concluded that the greater the water depth of a flat bottom, the slower the development of a sand spit, even if the same amount of sand is supplied from the upcoast, resulting in the decrease in the level of protrusion of the sand spit toward the X-axis from the point from which the elongation of the sand spit started. Furthermore, with the increase in the water depth of the flat bottom, the tip of the sand spit was forced to be bent landward, and it connected the X-axis at X = 10 m after 4 hr, while leaving a small lagoon behind the sand bar. In addition to this, the sand deposited upcoast of the sand spit quickly discharged downcoast after 4 hr, because the discontinuity of the shoreline at the tip of the sand spit disappeared, so that longshore sand transport was able to smoothly reach the downcoast shoreline. In Case 4 (h_0 = 20 cm), the development of the sand spit was further depressed and the scale of the sand spit was significantly reduced. Although a small hollow was formed behind the sand bar, no lagoon was formed.

After selecting the shoreline configurations of Cases 1-4 after 2 hr, each shoreline shape was compared with each other, as shown in Fig. 10. The shoreline upcoast of X = 8 m, where there is a sand source, coincides with each other. This means that the incident angle relative to the direction normal to the shoreline upcoast of X = 8 m is constant in each case, and therefore, the longshore sand transport also becomes constant because of the equivalence of the incident wave height, implying that the sand spit was formed under the condition that a constant volume of sand is supplied from the upcoast. In other words, the difference in the development of the sand spit must be explained only by the difference in the water depth of the flat shallow sea bottom. With the increase in the water depth, the sand spit was depressed, and a semicircular cuspate foreland was formed instead of a sand spit when the water depth of the flat shallow seabed is 20 cm.

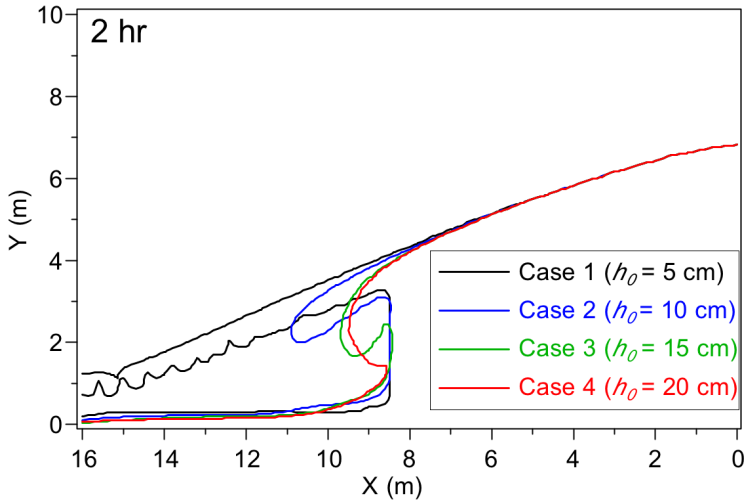

Figure 10. Shoreline configurations after 2 hr for Cases 1-4.

Formation of Sand Spit on Sloping Bed of tanβ = 1/50, 1/40, 1/30, and 1/20

The elongation of the sand spit on the sloping bed was also calculated while changing the seabed slope to tanβ = 1/50, 1/40, 1/30, and 1/20. Figure 11 shows the initial topography and its result when the seabed slope is 1/50. Because the seabed slope is as gentle as 1/50, the sand spit elongated in the same manner as that in Case 2 (h_0 = 10 cm), as shown in Fig. 7. The water depth at the tip of the sand spit increased with the elongation of the sand spit, and therefore, the sand spit did not extend in a straight manner and curved landward. The duration when the tip of the sand spit approached the other shore was 8 hr in Case 2, whereas in Case 5, it was only 4 hr. After 8 hr, a lagoon was left behind the sand bar, the depth of which increases in the X-direction, because the lagoon was enclosed by the barrier from the seaward side.

Figure 12 shows the results of Case 6 (tanβ = 1/40). They are similar to the results in Case 5, but comparison of the forms of the sand spits after 2 hr in Cases 5 and 6 shows that the length of the sand spit was reduced and the curvature of the sand spit increased in Case 6 compared with that in Case 5 because of the increase in the seabed slope from 1/50 to 1/40. Figures 13 and 14 show the results of Cases 7 and 8 (tanβ = 1/30 and 1/20); the elongation velocity further decreased and the curvature of the tip of the sand spit increased because of the increasing seabed slope. Therefore, the tip of the sand spit was almost connected to the other shore after 2 hr in Case 7, and it has already connected to the other shore in Case 8 within the same duration.

By selecting the shoreline after 2 hr in Cases 5-8, the shoreline in each case was superimposed as in Fig. 15. In these cases, also the longshore sand transport across the section of X = 8 m in each case is equivalent, because the shoreline in the area between X = 0 and 8 m, which is the source of sand supply, was completely superimposed, implying that the sand spit has been formed under the condition that the sand supply from the upcoast is constant. In other words, the difference in the elongation of a sand spit must be again explained only on the basis of the seabed slope in the sand deposition zone. Finally, it is concluded that with the increase in the seabed slope, the curvature near the tip of the sand spit increased and the tip was forced to approach the other shore. The most protruded location of the cuspate foreland, which was formed on the other shore owing to the wave-sheltering effect of the sand spit itself, was gradually moved deep in the bay with increasing seabed slope.

Figure 16 shows the change in cross section along transect A-A' at Y = 1.4 m in Cases 5-8. Along this transect, the change in cross section during the elongation of the sand spit to form a barrier can be studied. In Case 5, although a tiny triangular hump was formed after 2 hr at X = 11.5 m, a sand bar rapidly developed after 4 hr, and with time, the width of the barrier increased, leaving a large lagoon inside. In Cases 6 and 7, a subsurface sand bar of triangular shape was also formed after 2 hr, the crown height of the subsurface sand bar increased with the seabed slope, and in Case 8, the crown of the sand bar reached above sea level. Note that with the increase in the seabed slope, the area where the sand spit elongated was pushed landward, resulting in the narrowing of the lagoon inside. Thus, the gentler the seabed slope of the sand deposition zone, the more offshore the sand spit develops, with an increasing scale of the sand spit. Furthermore, note that the subsurface sand bar developed as a forerunner before the emergence of the sand spit over the sea surface.

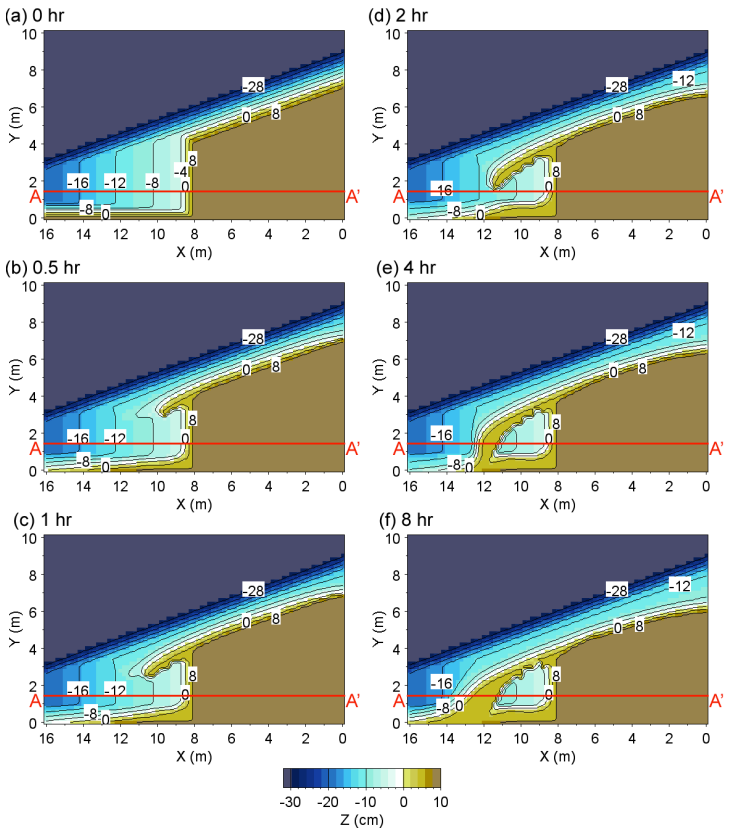

Figure 11. Formation of sand spit on sea bottom with 1/20 slope (Case 5).

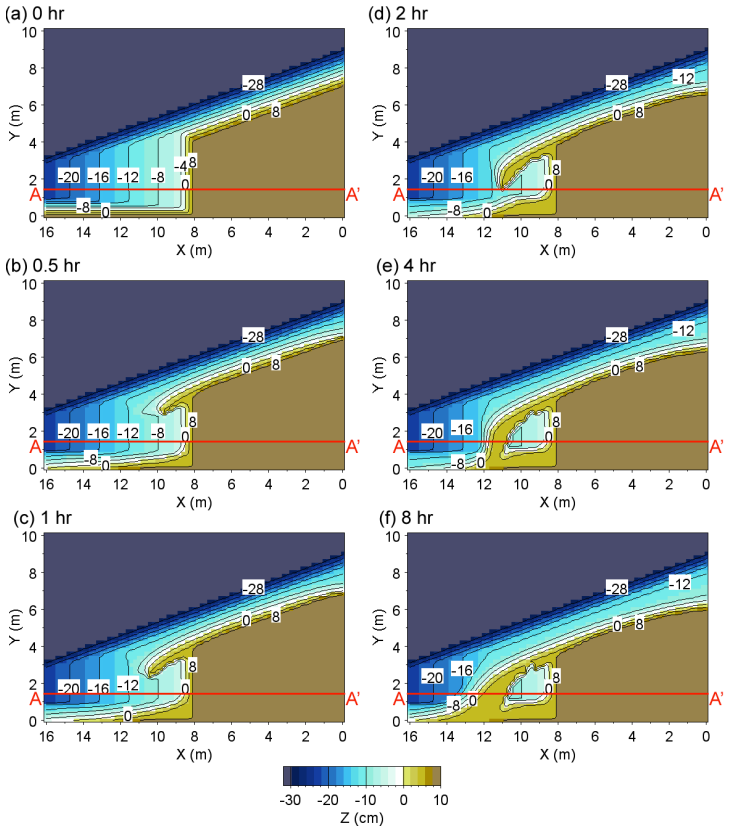

Figure 12. Formation of sand spit on sea bottom with 1/30 slope (Case 6).

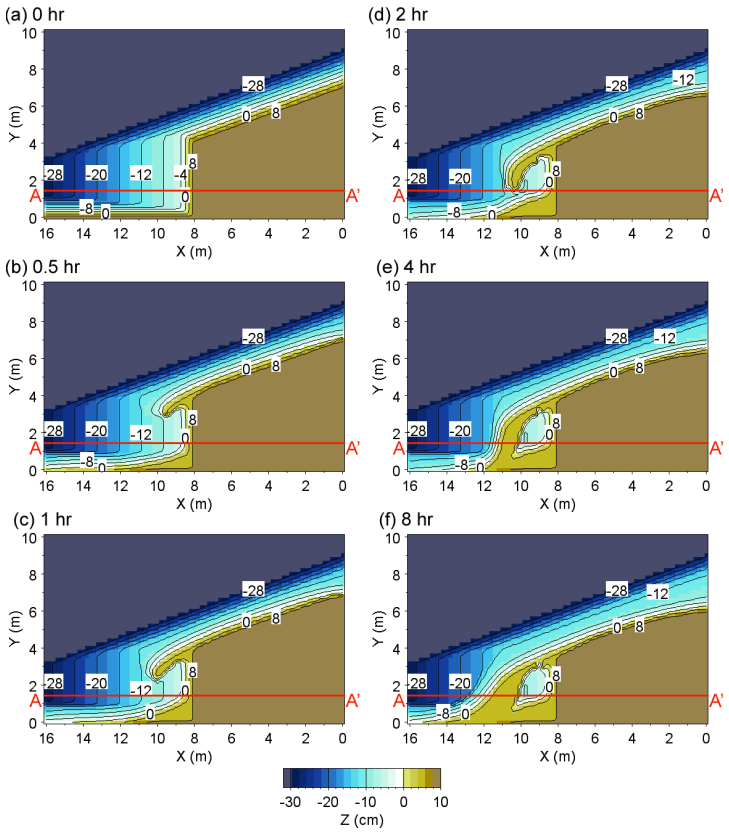

Figure 13. Formation of sand spit on sea bottom with 1/40 slope (Case 7).

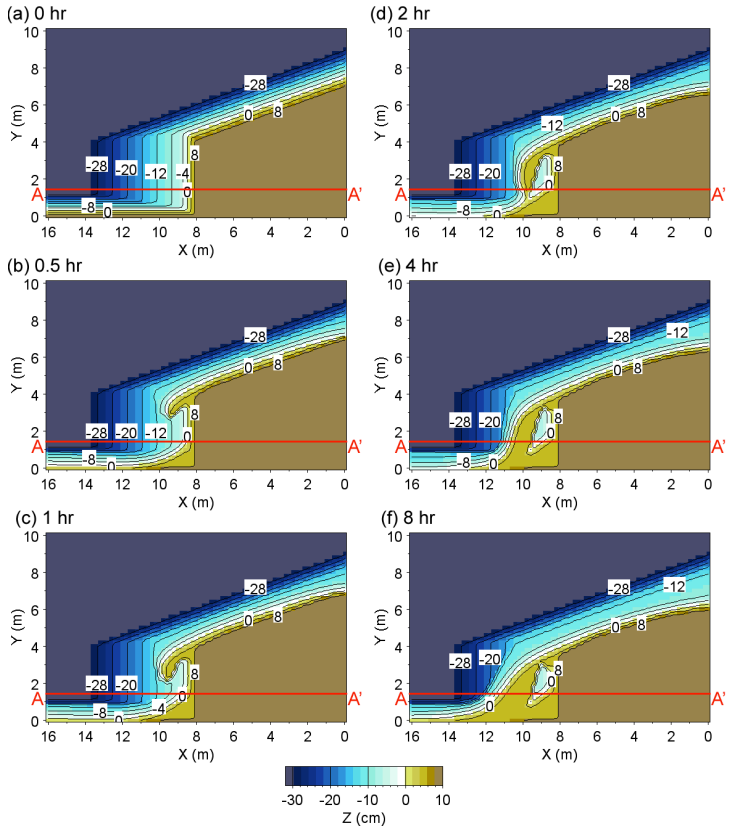

Figure 14. Formation of sand spit on sea bottom with 1/50 slope (Case 8).

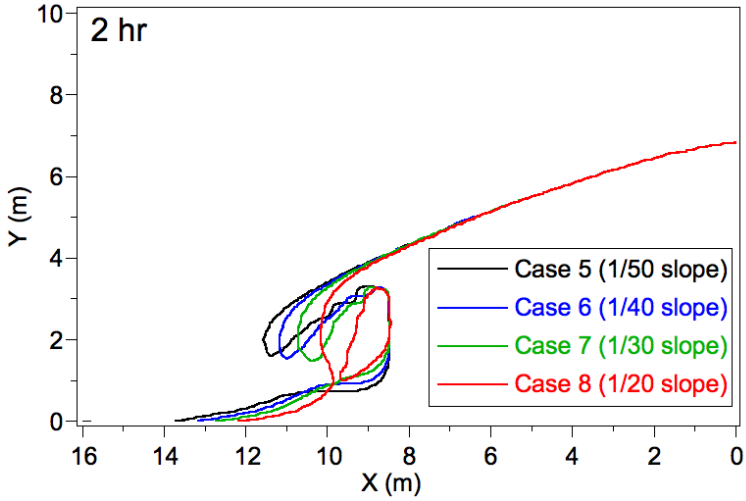

Figure 15. Shoreline configurations after 2 hr for Cases 5-8.

(a) Case 5 (1/50 slope)

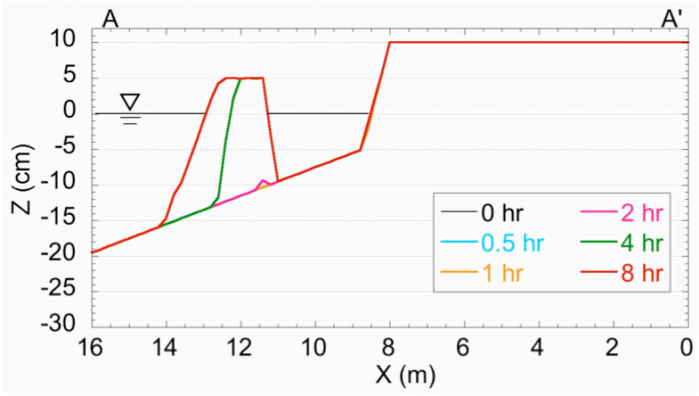

(b) Case 6 (1/40 slope)

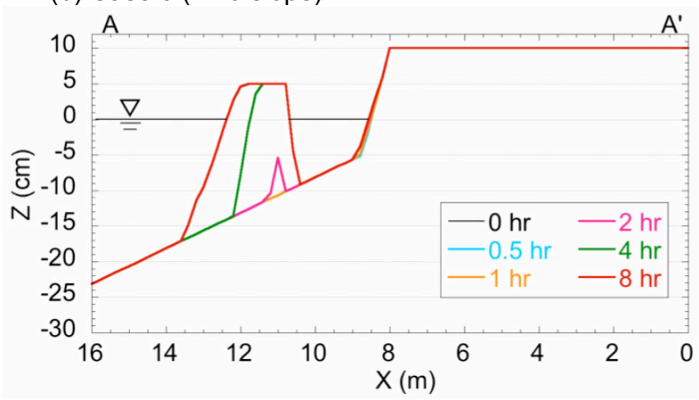

(c) Case 7 (1/30 slope)

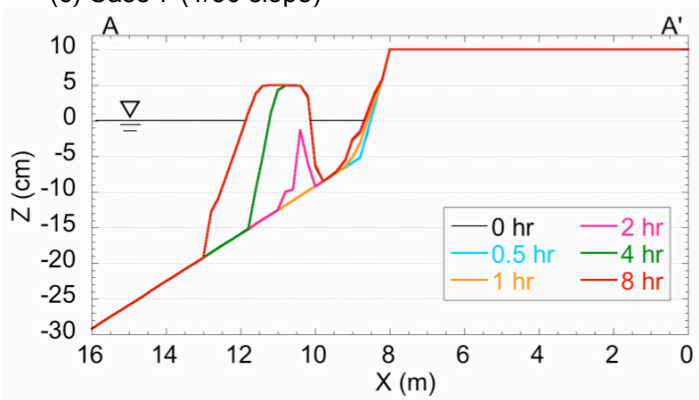

(d) Case 8 (1/20 slope)

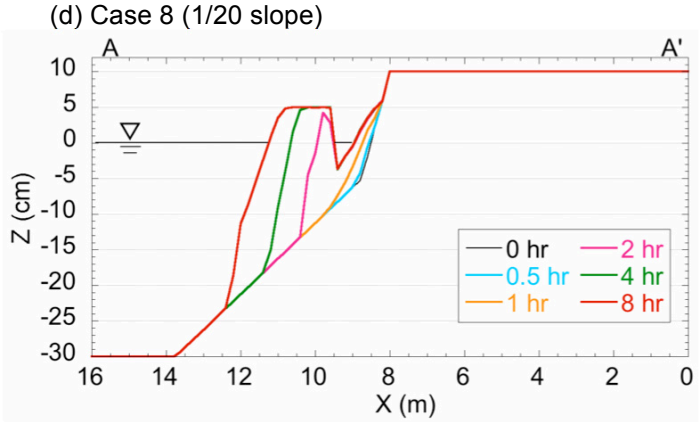

Figure 16. Profiles along transect Y = 1.4 m for Cases 5-8.

CONCLUSIONS

When a constant longshore sand transport Q_0 is supplied from upcoast and a sand spit is formed owing to this sand supply, the elongation velocity of the sand spit is proportional to Q_0/h^2, where h is the water depth of the sand deposition area. The development of the sand spit and a barrier as a result of the elongation of the sand spit is remarkable with a smaller water depth of the sand deposition zone. At the same time, sufficient wave energy cannot reach deep into the shallow body of water, inducing the development of a sand bar there, whereas sufficient wave energy can reach the shoreline with a larger water depth, resulting in the increase in the curvature of the shoreline. Mihama Point with a large water depth of the sand deposition area, which is much larger than the depth of closure of h_c =10 m, as shown in Fig. 2, is very similar to the results after 2 hr in Case 3 (Fig. 8d). The topography of Myojin Pond shown in Fig. 4 is similar to that after 8 hr in Case 2 (Fig. 7f), implying that Myojin Pond was left behind as a shallow pond, as a result of the extension of a slender barrier. In the case of Osezaki Point that protruded northward at the north end of Izu Peninsula (Fig. 5), the sand spit extended straight from the turning point of the coastline and then the tip of the sand spit recurved inward. This feature is similar to the result after 2 hr in Case 2 with a larger water depth of the flat seabed (Fig. 7d). The effect of the change in the seabed slope is equivalent to that of the combination of several flat seabeds. Thus, the results of the numerical simulations while changing the depth of the water body and seabed slope correspond well to the examples measured on coasts.

REFERENCES

Ashton, A. D., Murray, A. B. and Arnault, O. 2001. Formation of coastline features by large-scale instabilities induced by high-angle waves, *Nature*, 414, pp. 296-300.

Dally, W. R., Dean, R. G. and Dalrymple, R. A. 1984. A model for breaker decay on beaches, *Proc. 19th Int. Conf. Coastal Eng*., pp. 82-97.

Goda, Y. 1985. *Random Seas and Design of Maritime Structures*, University of Tokyo Press, Tokyo, p. 323.

Mase, H. 2001. Multidirectional random wave transformation model based on energy balance equation, *Coastal Eng. J.*, JSCE, 43(4), pp. 317-337.

Ozasa, H. and Brampton, A. H. 1980. Model for predicting the shoreline evolution of beaches backed by seawalls, *Coastal Eng*., 4, pp. 47-64.

Serizawa, M. and Uda, T. 2011. Prediction of formation of sand spit on coast with sudden change using improved BG model, *Coastal Sediments'11*, pp. 1907-1919.

Uda, T., Serizawa, M. and Miyahara, S. 2012. BG model based on Bagnold's concept and its application to analysis of elongation of sand spit and shore - normal sand bar (Chap. 16), in '*Numerical Simulation - From Theory to Industry*' Andriychuk, M. ed., INTEC, pp. 339-374. http://www.intechopen.com/books/numerical-simulation-from-theory-to-industry/bg-model-based-on-bagnold-s-concept-and-its-application-to-analysis-of-elongation-of-sand-spit-and-s

Uda, T., Gibo, M., Ishikawa, T., Miyahara, S., San-nami, T. and Serizawa, M. 2013. Change in carbonate beach triggered by construction of a bridge on Irabu Island and its simulation using BG model, *Asian and Pacific Coasts 2013, Proc. 7th International Conf*., pp. 24-31.